Journal of Engineering Sciences
Vol 11, Issue 3, March/2020
ISSN NO:0377-9254

FLC BASED BIDIRECTIONAL DC/DC CONVERTER WITH DUAL-BATTERY ENERGY STORAGE FOR HYBRID ELECTRIC VEHICLE SYSTEM

R. Durga Rao

Asst. Professor & Head, Department of EEE.JNTUH COLLEGE OF ENGINEERING MANTHANI.

durgarao@jntuh.ac.in

ABSTRACT- ***This paper describes about controlling of bidirectional DC-DC converter with Dual-Battery energy storage for electric vehicle applications by using fuzzy logic controller. The proposed converter operation classified into two modes i.e. Battery charging mode and battery discharging mode. In charging mode main energy system supplies to load and also delivers power to the rechargeable energy storage systems and in discharging mode all input sources deliver power to output. The proposed converter is used for controlling the power of ESSs by allowing active power sharing. The voltage levels of utilized ESSs can be higher or lower than the output voltage. By using the fuzzy controller for a nonlinear system allows for a reduction of uncertain effects in the system control and improves the efficiency.***

Keywords- BFEV- *Battery fed electric vehicles,* ***HEV-****Hybrid electric vehicles,*

INTRODUCTION

Recently bi-directional dc-dc converters are widely researched and developed for various applications such as battery charger-dischargers, electric vehicles and UPS systems. In case of the battery fed electric vehicles (BFEVs), electric energy flows between motor and battery side. For achieving zero emission, the vehicle can be powered only by batteries or other

Electrical energy sources. Batteries have widely been adopted in ground vehicles due to their characteristics in terms of high energy density, compact size, and reliability. This can be applied in Hybrid Electric Vehicle (HEVs) with a battery as an energy storage element to provide desired management of the power flows. In hybrid electric vehicle energy storage devices act as catalysts to provide energy boost. However the high initial cost of BFEVs as well as its short driving range has limited its use. Bidirectional dc-dc converters are the key components of the traction systems in Hybrid Electric Vehicles. The use of a Bi-directional dc-dc converter fed dc motor drive devoted to electric vehicles (EVs) application allows a suitable control of both motoring and regenerative braking operations, and it can contribute to a significant increase the drive system overall efficiency.

A functional diagram for a typical (FCV/HEV) power system is illustrated in Fig. 1 [4, 13]. The low-voltage FC stack is used as the main power source, and SCs directly connected in parallel with FCs. The dc/dc power converter is used to convert the FC stack voltage into a sufficient dc-bus voltage in the driving inverter for supplying power to the propulsion motor. Furthermore, ES1 with rather higher voltage is used as the main battery storage device for supplying peak power, and ES2 with rather lower voltage could be an auxiliary battery storage device to achieve the vehicle range extender concept [13]. The function of the bidirectional dc/dc converter (BDC) is to interface dual-battery energy storage with the dc-bus of the driving inverter

Journal of Engineering Sciences
Vol 11, Issue 3, March/2020
ISSN NO:0377-9254

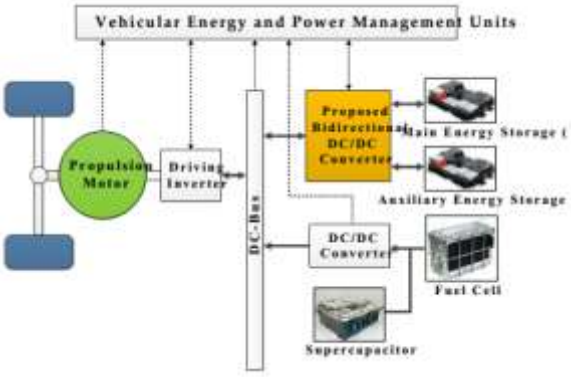

Fig. 1. Typical functional diagram for a FCV/HEV power system

Generally, the FC stack and battery storage devices have different voltage levels. Several multiport BDCs have been developed to provide specific voltages for loads and control power flow between different sources, thus reducing overall cost, mass, and power consumption [14-27]. These BDCs can be categorized into isolated and non isolated types.

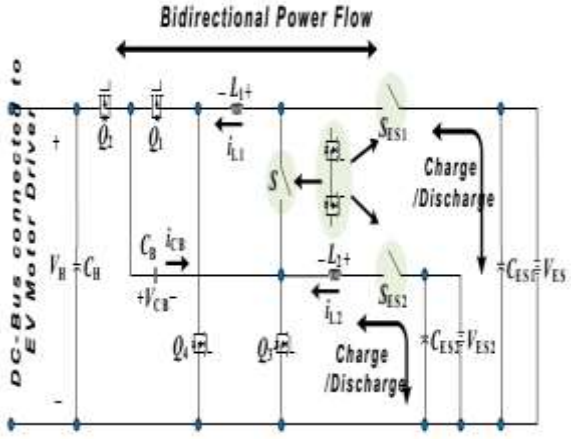

Fig.2.Proposed BDC topology with dual-battery energy storage

The proposed BDC topology with dual-battery energy storage is illustrated in Fig. 2, where VH, VES1, and VES2 represent the high-voltage dc-bus voltage, the main energy storage (ES1), and the auxiliary energy storage (ES2) of the system, respectively. Two bidirectional power switches (SES1 and SES2) in the converter structure, are used to switch on or switch off the current loops of ES1 and ES2, respectively. A charge-pump capacitor (CB) is integrated as a voltage divider with four active switches (Q1, Q2, Q3, Q4) and two phase inductors (L1, L2) to improve the static voltage gain between the two low-voltage dual sources (VES1, VES2) and the high-voltage dc bus (VH) in the proposed converter. Furthermore, the additional CB reduces the switch voltage stress of active switches and eliminates the need to operate at an extreme duty ratio. Furthermore, the three bidirectional power switches (S, SES1, SES2) displayed in Fig. 2 exhibit four-quadrant operation and are adopted to control the power flow between two low-voltage dual sources (VES1, VES2) and to block either positive or negative voltage. This bidirectional power switch is implemented via two metal-oxide-semiconductor field-effect transistors (MOSFETs), pointing in opposite directions, in series connection. To explain the concept for the proposed converter, all the conduction statuses of the power devices involved in each operation mode are displayed in Table I. Accordingly, the four operating modes are illustrated as follows to enhance understanding.

TABLE I
CONDUCTION STATUS OF DEVICES FOR DIFFERENT OPERATING MODES

Operating Modes	ON	OFF	Control Switch	Synchronous Rectifier (SR)
Low-voltage dual-source-powering mode (Accelerating, x_1=1, x_2=1)	S_{SES1}, S_{SES2}	S	Q_3, Q_4	Q_1, Q_2
High-voltage dc-bus energy-regenerating mode (Braking, x_1=1, x_2=1)	S_{SES1}, S_{SES2}	S	Q_1, Q_2	Q_3, Q_4
Low-voltage dual-source buck mode (ES1 to ES2, x_1=0, x_2=0)	S_{SES1}, S_{SES2}	Q_1, Q_2, Q_3	S	Q_4
Low-voltage dual-source boost mode (ES2 to ES1, x_1=0, x_2=0)	S_{SES1}, S_{SES2}	Q_1, Q_2, Q_4	Q_3	S
System shutdown	-	S_{SES1}, S_{SES2} Q_1, Q_2, Q_3, Q_4	-	-

And to block either positive or negative voltage. This bidirectional power switch is implemented via two metal-oxide-semiconductor field-effect transistors (MOSFETs), pointing in opposite directions, in series connection.

To explain the concept for the proposed converter, all the conduction statuses of the power devices involved in each operation mode are displayed in Table I. Accordingly; the four operating modes are illustrated as follows to enhance understanding.

A. Low-Voltage Dual-Source-Powering Mode

Fig. 3(a) depicts the circuit schematic and steady-state waveforms for the converter under the low-voltage dual-source-powering mode. Therein, the switch S is turned off, and the switches (SES1, SES2) are turned on, and the two low-voltage dual sources (VES1, VES2) are supplying the energy to the dc-bus and loads. In this mode, the low-side switches Q3and Q4are actively switching at a phase-shift angle of 180° , and the high-side switches Q1 and Q2 function as the synchronous rectifier (SR).

Based on the typical waveforms shown in Fig. 3(b), when the duty ratio is larger than 50%, four circuit states are possible (Fig. 4). In the light of the on/off status of the active switches and the operating principle of the BDC in low-voltage dual-source-powering mode, the operation can be explained briefly as follows.

State 1 [t0 < t < t1]: During this state, the interval time is (1-Du)T_{sw}, switches Q1, Q3are turned on, and switchesQ2, Q4 are turned off. The voltage across L1is the difference between the low-side voltage VES1and the charge-pump voltage (VCB), and hence iL1 decreases linearly from the initial value. In addition, inductor L_2 is charged by the energy source VES2,

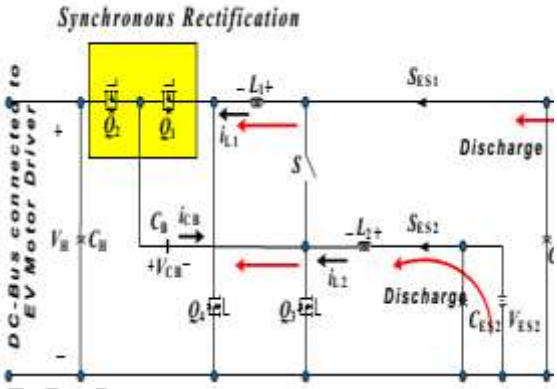

Fig 3: Low-voltage dual-source-powering mode of the proposed BDC

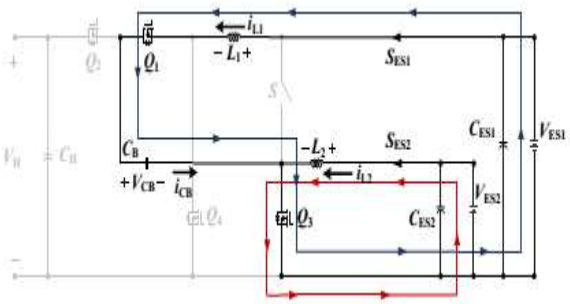

(a)

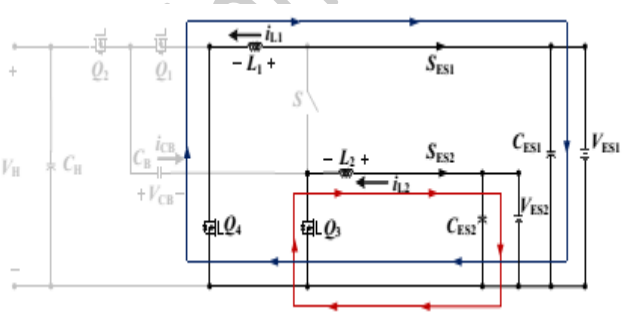

(b)

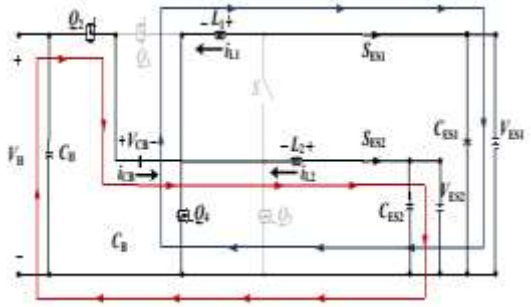

(c)

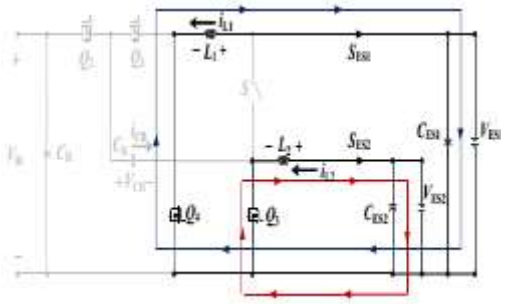

(d)

Fig. 4. Circuit states of the proposed BDC for the high-voltage dc-bus energy-regenerating mode. (a) State 1. (b) State 2. (c) State 3. (d) State 4.

a) State 1 [t0 < t < t1]: During this state, the interval time is Dd Tsw; switches Q1and Q3 are turned on, and switchesQ2and Q4 are turned off. The voltage across L1is the difference between the low-side voltage VES1 and the charge-pump voltage VCB; hence, the inductor current iL1 decreases linearly from the initial value. In addition, inductor L2is charged by the energy source VES2, which also contributes to the linear increase in the inductor current. The voltages across inductors L1and L2can be denoted as

$$L_1 \frac{di_{L1}}{dt} = V_{ES1} - V_{CB} \quad (9)$$

$$L_2 \frac{di_{L2}}{dt} = V_{ES2}$$

b) State 2 [t1 < t < t2]: During this state, the interval time is (0.5-Dd) T_{sw}; switches Q3and Q4 are turned on, and switchesQ1 and Q2are turned off. The voltages across inductors L1 andL2 are the positive the low-side voltages VES1and VES2, respectively; hence, inductor currents iL1 and iL2 increase linearly. These voltages can be denoted as

$$L_1 \frac{di_{L1}}{dt} = V_{ES1}$$

$$L_2 \frac{di_{L2}}{dt} = V_{ES2}$$

c) State 3 [t2 < t < t3]: During this state, the interval time is Dd T_{sw}; switches Q1 and Q3 are turned off, and switchesQ2and Q4are turned on. The voltage across L1is the positive low-side voltage VES1 and hence iL1 increases linearly from the initial value. Moreover, the voltage across L2is the difference of the high-side voltage VH, the charge-pump voltage VCB, and the low-side voltage VES2, and its level is negative. The voltages across inductors L1and L2can be denoted as

d) State 4 [t3 < t < t4]: During this state, the interval time is (0.5-Dd)Tsw; switches Q3and Q4 are turned on, and switchesQ1 and Q2are turned off. The voltages across inductors L1and L2 can be denoted as,

$$L_1 \frac{di_{L1}}{dt} = V_{ES1}$$

$$L_2 \frac{di_{L2}}{dt} = V_{ES2}$$

C. Low-Voltage Dual-Source Buck/Boost Mode

The circuit schematic for this mode, which involves the transfer of energy stored in the main energy storage to the auxiliary energy storage and vice versa is presented in Fig. 7. Therein, the topology is converted into a single-leg bidirectional buck-boost converter.

As shown in Fig. 8, when the duty cycle of the active bidirectional switch S is controlled, the buck converter channels power from main energy storage to the auxiliary energy storage. By contrast, when the duty cycle of switch Q3 is controlled, power flows from the auxiliary energy storage to main energy storage, indicating that the converter is operating in boost mode, as illustrated in Fig.9.

CONVERTER CONTROL

Fig. 10(a) depicts the converter control structure, which consists of a vehicular strategic management level and the proposed BDC controller. The corresponding realized DSP flowchart for selecting operating modes of the proposed BDC is also shown in Fig. 10(b) for reference.

The strategic management level involves electrical power demand estimation and contains a vehicular power and voltage management unit. The global results of the management must maximize the use of the source that best suits the power train power demand, fulfilling the driver and route requirements [21, 25-33]. In FCV/HEV power systems (Fig. 1), the

dc-bus voltage of the driving inverter is regulated and powered by the FC stack through a dc-dc converter. Hence, instead of controlling the converter output voltage of each operation mode, the inductor current iL1or iL2is detected and compared with the reference current to control the power flow as shown in Fig. 10(a).

In the converter control structure, the vehicular energy and power and voltage management unit selects the BDC mode according to the operating conditions of the vehicle, such as power demand of different driving state (P_{dem}) and the dual-source voltages (VES1, VES2).It then selects the appropriate current references iL1,re for iL2,refthat can control the active switches (S, Q1~Q4) with proportional integral (PI) or more advanced methods. Notably, in spite of it is not easy to choose the optimal parameter of PI controller, the advantages of zero steady-state error and capability of noise filtering, making PI control the most widely used industry algorithm. Furthermore, referring to Table I, two switch selector (x1, x2) of BDC controller can be defined for various operating modes. The pulsed-width-modulation (PWM) switching scheme converts the duty cycle determined by different switch selector statuses into gate control signals for the power switches.

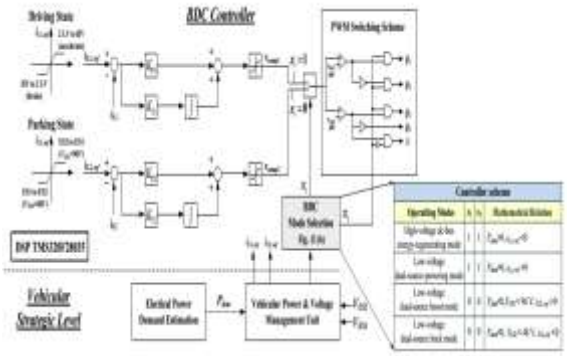

(a)

As Fig. 10(a) displays, the current reference $i_{L1,ref}$ is used to control the bidirectional power flow between the low-voltage dual-source and the high-voltage dc-bus (i.e., 2 LV to HV or HV to 2 LV). In either case, the average inductor current iL2 is equal to the controlled average inductor current iL1 because of the inherent uniform average current sharing in the proposed BDC topology. By contrast, the current reference $i_{L2,ref}$ is used to control the power flow between the main energy storage and the auxiliary energy storage (i.e., ES1 to ES2 or ES2 to ES1).

The procedure of mode switching is shown in Fig. 10(b) and it is depicted below. First of all, when vehicle is in driving state (P_{dem}>0), the controller is iL1 control loop (x1=1), and the controlled switches as shown in Table I (vehicle is accelerating (iL1,ref >0, HV to 2 LV) or braking (iL1,ref<0, 2 LV to HV)). If neither of the two situations, it will execute reselect mode to process the next judgment of mode switching. Additionally, when vehicle is in parking state (P_{dem}<0), the controller is iL2 control loop (x1=0), and controlled switches as shown in Table I.

(b)**Fig. 5. (a) Block diagram of the closed-loop control scheme; (b) realized DSP flowchart for various operating modes of the proposed BD C.**

In this state, the judgment of mode switching depends on the voltage of VES1(96 V) and VES2(48 V). If VES1<96V, the mode is low-voltage dual-source boost mode ($i_{L2,ref}$ >0, VES2 to VES1). When VES2<48 V, the mode is low-voltage dual-source buck mode (iL2,ref <0, VES1 to VES2). If both situations do not be satisfied, it executes reselect mode to process the next

FUZZY LOGIC CONTROLLER

Fuzzy logic control mostly consists of three stages: a) Fuzzification b) Rule base c) Defuzzification During fuzzification, numerical input variables are converted into linguistic variable based on a membership functions. For these MPP techniques the inputs to fuzzy logic controller are taken as a change in power w.r.t change in current E and change in voltage error C. Once E and C are calculated and converted to the linguistic variables, the fuzzy controller output, which is the duty cycle ratio D of the power converter, can be search for rule base table. The variables assigned to D for the different combinations of E and C is based on the intelligence of the user. .

Architecture of Fuzzy Logic Controller : The architecture of the fuzzy logic controller shown in Fig. 3 includes four components: Fuzzifier, Rule Base, Fuzzy Inference Engine (decision making unit), and Defuzzifier.

Fuzzifier: Fuzzy logic uses linguistic variables instead of numerical variables. In a control system, error between reference signal and output signal can be assigned as Negative Big (NB), Negative Medium (NM), Negative Small (NS), Zero (ZE), Positive small (PS), Positive Medium (PM), Positive Big (PB). The triangular membership function is used for fuzzifications. The process of fuzzification convert numerical variable (real number) to a linguistic variable (fuzzy number) so that it can be matched with the premises of the fuzzy rules defined in the application specific rule base.

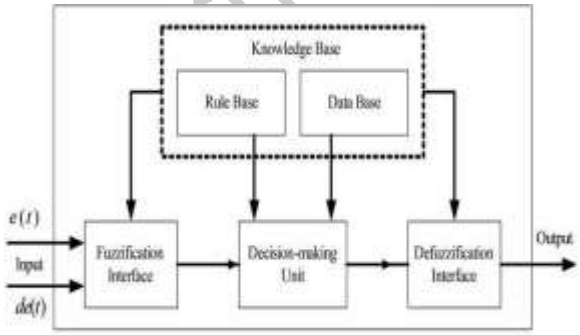

Fig. 6 Architecture of Fuzzy Logic Controller

Table. 2 The Membership Functions For FLC

The rule base contains a set of fuzzy if-then rules which defines the actions of the controller in terms of linguistic variables and membership functions of linguistic terms. The Rule base stores the linguistic control rules required by rule evaluator (decision making logic).The output of the fuzzy controller is estimating the magnitude of peak reference current. This peak reference current comprises active power demand of the non-linear load and losses in the distribution system. The peak reference current is multiplied with PLL output for determining the desired reference current. Database: The Database stores the definition of the triangular membership function required by fuzzifier and defuzzifier.

Fuzzy Inference Engine: The fuzzy inference engine applies the inference mechanism to the set of rules in the fuzzy rule base to produce a fuzzy output set. This involves matching the input fuzzy set with the premises of the rules, activation of the rules to deduce the conclusion of each rule that is fired, and combination of all activated conclusions using fuzzy set union to generate fuzzy set output.

Defuzzifier: The rules of fuzzy logic controller generate required output in a linguistic variable (Fuzzy Number), according to real world requirements; linguistic variables have to be transformed to crisp output (Real number). This selection of strategy is a compromise between accuracy and computational intensity.

variables area unit outlined as (NB, NM, NS, Z, PS,PM, PB) that means negative big, negative medium, negative small, zero, positive small, positive medium and positive big

E CE	NB	NM	NS	Z	PS	PM	PB
PB	Z	PS	PM	PB	PB	PB	PB
PM	NS	Z	PS	PM	PB	PB	PB
PS	NM	NS	Z	PS	PM	PB	PB
Z	NB	NM	NS	Z	PS	PM	PB

SIMULATION RESULTS

Simulations and experiments were conducted to verify the performance of the proposed model. A photograph of the realized BDC prototype and the test bench are shown in Fig.below. DC voltage sources and electric loads were substituted for the main energy storage and the auxiliary energy storage. The system developed in this study included two loads for the high-voltage dc-bus energy-regenerating mode and two sources for the low-voltage dual-source-powering mode.

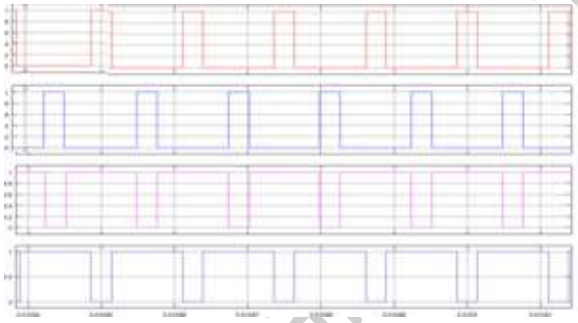

7(a)

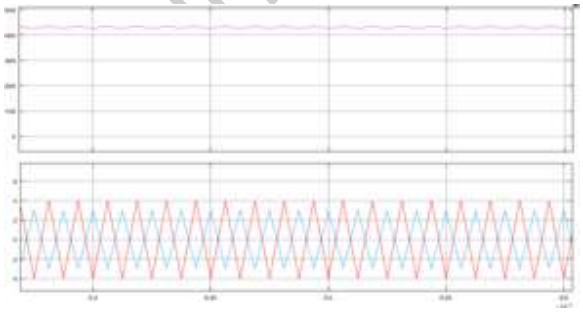

Fig. 7.Measured waveforms for low-voltage dual-source-powering mode: (a) gate signals; (b) output voltage and inductor currents.

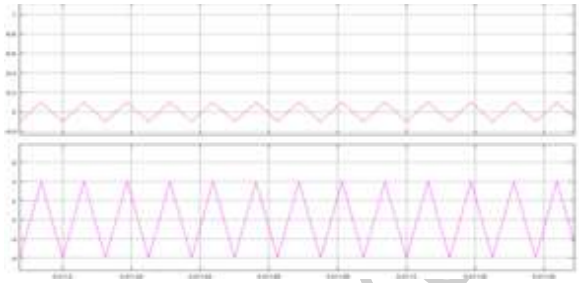

8(a)

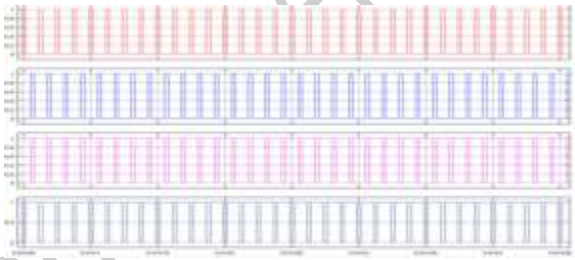

Fig. 8.Measured waveforms for high -voltage dual-source-powering mode: (a) gate signals; (b) output voltage and inductor currents.

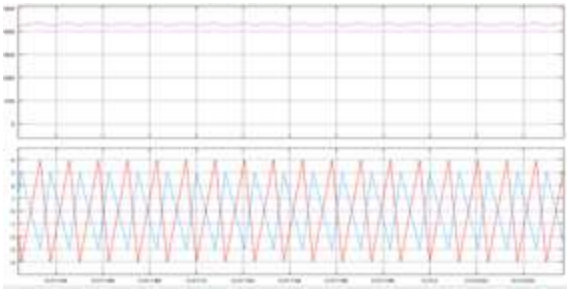

9(a)

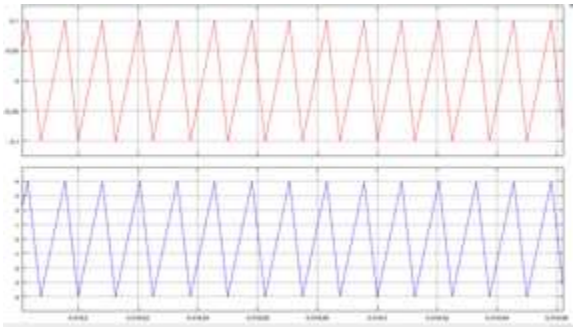

9(b) . Waveforms of controlled current step change in the low-voltage dual-source-powering mode: (a) by

simulation; and (b) by measurement. (*iH* is changed from 0 to 0.85 A; *iL*1 is changed from 0 to 2.5 A; Time/Div=20 ms/Div)

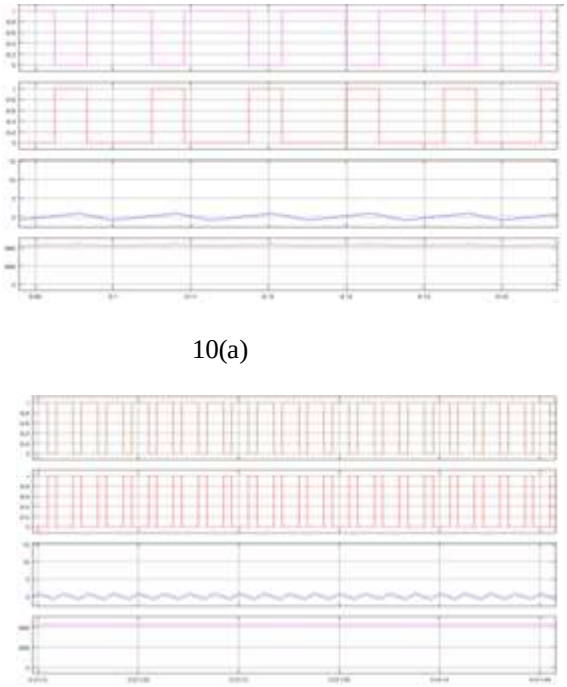

10(a)

Fig.10. Measured waveforms of gate signals, output voltage and inductor currents for the low-voltage dual-source buck/boost mode: (a) buck mode; (b) boost mode.

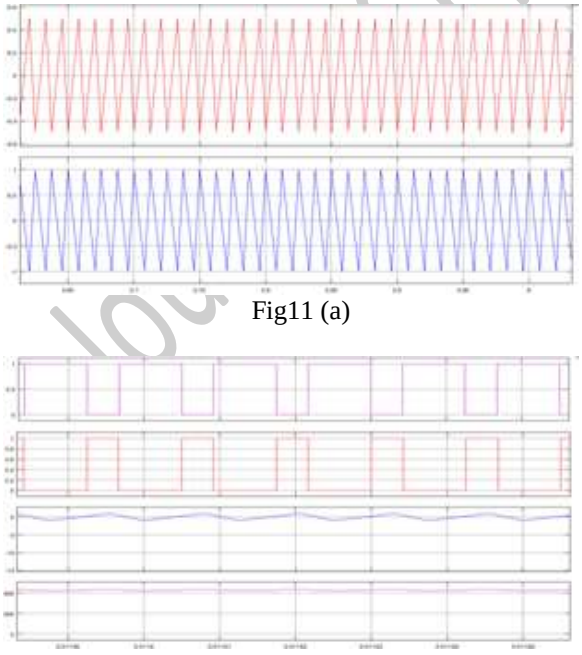

Fig11 (a)

Fig.11(b). Waveforms of controlled current step change in the high-voltage dc-bus energy-regenerating mode: (a) by simulation; and (b) by measurement. (*iH* is changed from 0 to -0.85 A; *iL*1 is changed from 0 to -2.5 A; Time/Div=20 ms/Div)

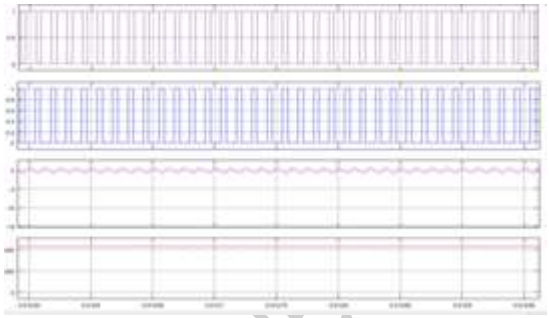

12(a)

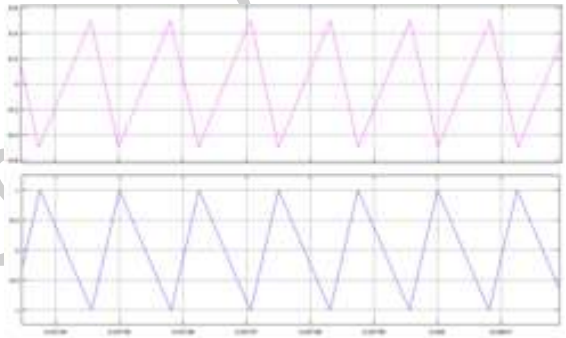

Fig12 (b) Waveforms of controlled current step change in the low-voltage dual- source buck mode: (a) by simulation; and (b) by measurement. (*iES*1 is changed from 0 to 6 A; *iL*2 is changed from 0 to 12 A; Time/Div=20 ms/Div)

CONCLUSIONS

Fuzzy logic controller provides fewer fluctuations as compared with previous controller. It maintains less THD values and gives more efficiency. Because of using rule base Technique it measures errors more accurately as compared with conventional controller(PI).

REFERENCES

[1] M. Ehsani, K. M. Rahman, and H. A. Toliyat, "Propulsion system design of electric and hybrid vehicles," IEEE Transactions on industrial electronics, vol. 44, no. 1, pp. 19-27, 1997.

[2] A. Emadi, K. Rajashekara, S. S. Williamson, and S. M. Lukic, "Topological overview of hybrid electric and fuel cell vehicular power system architectures and configurations," IEEE Transactions on Vehicular Technology, vol. 54, no. 3, pp. 763-770, 2005.

[3] A. Emadi, S. S. Williamson, and A. Khaligh, "Power electronics intensive solutions for advanced electric, hybrid electric, and fuel cell vehicular power systems," IEEE Transactions on Power Electronics, vol. 21, no. 3, pp. 567-577, 2006.

[4] E. Schaltz, A. Khaligh, and P. O. Rasmussen, "Influence of battery/ultracapacitor energy-storage sizing on battery lifetime in a fuel cell hybrid electric vehicle," IEEE Transactions on Vehicular Technology, vol. 58, no. 8, pp. 3882-3891, 2009.

[5] P. Thounthong, V. Chunkag, P. Sethakul, B. Davat, and M. Hinaje, "Comparative study of fuel-cell vehicle hybridization with battery or super capacitor storage device," IEEE transactions on vehicular technology, vol. 58, no. 8, pp. 3892-3904, 2009.

[6] C. C. Chan, A. Bouscayrol, and K. Chen, "Electric, hybrid, and fuel-cell vehicles: Architectures and modeling," IEEE transactions on vehicular technology, vol. 59, no. 2, pp. 589-598, 2010.

[7] A. Khaligh and Z. Li, "Battery, ultra capacitor, fuel cell, and hybrid energy storage systems for electric, hybrid electric, fuel cell, and plug-in hybrid electric vehicles: State of the art," IEEE transactions on Vehicular Technology, vol. 59, no. 6, pp. 2806-2814, 2010.

[8] K. Rajashekara, "Present status and future trends in electric vehicle propulsion technologies," IEEE Journal of Emerging and Selected Topics in Power Electronics, vol. 1, no. 1, pp. 3-10, 2013.

[9] C.-M.Lai, Y.-C. Lin, and D. Lee, "Study and implementation of a two-phase interleaved bidirectional DC/DC converter for vehicle and dc-microgrid systems, " Energies, vol. 8, no. 9, pp. 9969-9991, 2015.

[10] C.-M. Lai, "Development of a novel bidirectional DC/DC converter topology with high voltage conversion ratio for electric vehicles and DC-microgrids," Energies, vol. 9, no. 6, p. 410, 2016.

[11] J. Moreno, M. E. Ortúzar, and J. W. Dixon, "Energy-management system for a hybrid electric vehicle, using ultracapacitors and neural networks," IEEE transactions on Industrial Electronics, vol. 53, no. 2, pp. 614-623, 2006.

[12] J. Bauman and M. Kazerani, "A comparative study of fuel-cell–battery, fuel-cell–ultracapacitor, and fuel-cell–battery–ultracapacitor vehicles," IEEE Transactions on Vehicular Technology, vol. 57, no. 2, pp. 760-769, 2008.

[13] M. Ehsani, Y. Gao, and A. Emadi, Modern electric, hybrid electric, and fuel cell vehicles: fundamentals, theory, and design . CRC press, 2009.